

INFA-GUARD: Mitigating Malicious Propagation via Infection-Aware Safeguarding in LLM-Based Multi-Agent Systems

Yijin Zhou^{1,2,3,*}, Xiaoya Lu^{1,2,*}, Dongrui Liu^{2,†}, Junchi Yan^{1,3}, Jing Shao^{2,†}

¹Shanghai Jiao Tong University, China

²Shanghai Artificial Intelligence Laboratory, China

³Shanghai Innovation Institute, China

Abstract

The rapid advancement of Large Language Model (LLM)-based Multi-Agent Systems (MAS) has introduced significant security vulnerabilities, where malicious influence can propagate virally through inter-agent communication. Conventional safeguards often rely on a binary paradigm that strictly distinguishes between benign and attack agents, failing to account for infected agents *i.e.*, benign entities converted by attack agents. In this paper, we propose **Infection-Aware Guard**, INFA-GUARD, a novel defense framework that explicitly identifies and addresses infected agents as a distinct threat category. By leveraging infection-aware detection and topological constraints, INFA-GUARD accurately localizes attack sources and infected ranges. During remediation, INFA-GUARD replaces attackers and rehabilitates infected ones, avoiding malicious propagation while preserving topological integrity. Extensive experiments demonstrate that INFA-GUARD achieves state-of-the-art performance, reducing the Attack Success Rate (ASR) by an average of 33%, while exhibiting cross-model robustness, superior topological generalization, and high cost-effectiveness.

Warning: this paper includes examples that may be misleading or harmful.

1 Introduction

The remarkable evolution of Large Language Models (LLMs) (Brown et al., 2020; Achiam et al., 2023; Guo et al., 2025) has catalyzed a paradigm shift from standalone models to autonomous agents. The pursuit of more advanced problem-solving has naturally led to the development of Multi-Agent Systems (MAS) (Yan et al., 2025). By enabling specialized agents to communicate and collaborate,

MAS establishes powerful cooperative frameworks that have proven highly effective (Kim et al., 2024; Borghoff et al., 2025).

While such interconnectivity empowers MAS, it introduces profound security challenges beyond single-agent systems (Dong et al., 2024; Yu et al., 2025). Security risks are no longer localized. Instead, misleading information and erroneous behaviours in several agents can propagate through inter-agent interactions, catalyzing systemic decision failure (Ju et al., 2024; Zheng et al., 2025). Specifically, such propagation is typically initiated by the strategic insertion of attack agents. Attacks deliberately employ persuasive yet deceptive arguments (Agarwal and Khanna, 2025), disseminate falsehoods (Ju et al., 2024), or introduce malicious tools (Zhan et al., 2024) to manipulate connected benign agents, ultimately steering MAS toward an incorrect consensus (Zheng et al., 2025). The malicious propagation hinges on a dynamic conversion as illustrated in Fig. 1(a): **attack agents** persuade **benign agents**, converting them into **infected agents** that output erroneous conclusions.

The existing safeguards for MAS have operated under a binary paradigm, distinguishing strictly between **benign agents** and **attack agents** (Wang et al., 2025c; Miao et al., 2025; Wu et al., 2025; Feng and Pan, 2025). However, they overlook the distinct characteristics and behaviors of the originating attack agents and the resulting infected agents. As illustrated in Fig. 1(b), this binary oversimplification leads to the oversight of infected agents, limiting the effectiveness of safeguards in two ways (Section 3): (1) **Infected agents are harmful information propagators**. Even if the attack agent's communication channels are later severed, the already-infected agents can continue to disseminate harmful information. (2) **Ignoring infected agents leads to forfeiting topological constraint information**. An infected agent significantly increases the probability of finding an attack agent in its neighborhood,

*Equal contribution.

†Corresponding authors:

liudongrui@pjlab.org.cn, shaojing@pjlab.org.cn.
Code – <https://github.com/yjzscode/INFA-Guard>

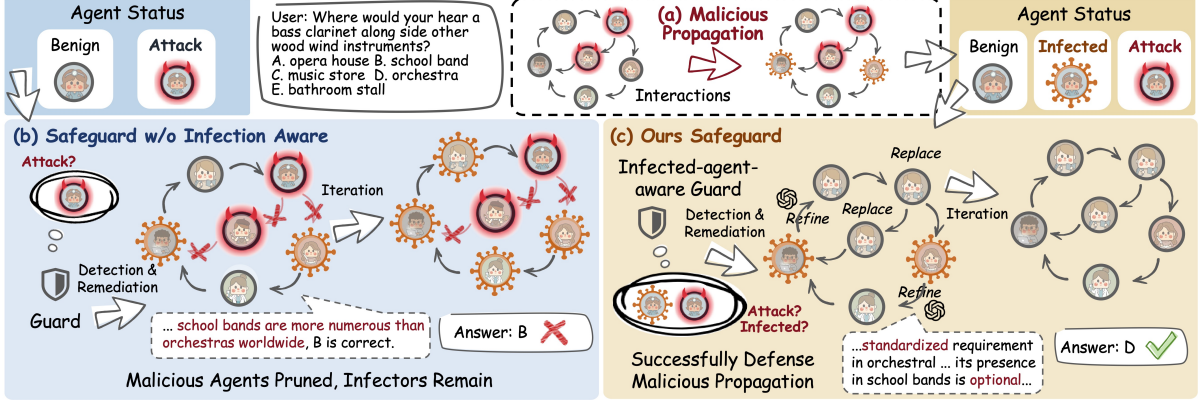


Figure 1: The paradigm comparison between existing MAS safeguards and our infection-aware safeguard.

and vice versa. Consequently, by neglecting the detection and modeling of infected agents, existing safeguards fail to leverage this mutual relationship.

In this paper, we are the first to address infected agents as a distinct threat category in MAS security, with empirical validation of the necessity and importance, and understanding of the malicious information propagation dynamics. We propose a novel defense method for MAS, termed INFA-GUARD. It processes attack and infected agents as shown in Fig. 1(c). For detection, INFA-GUARD employs a specialized network architecture and topological constraints to iteratively identify both attack and infected agents by modeling the dynamic infection process. For remediation, based on the distinct characteristics of attack agents and infected agents and their topology constraints, we replace attack agents while refining infected ones.

By coupling accurate detection with targeted remediation, INFA-GUARD effectively ensures system security while preserving the response diversity and topological integrity of MAS. Extensive experiments demonstrate that INFA-GUARD significantly reduces the Attack Success Rate (ASR), outperforming baselines by an average of 4.5% and up to 12.9% across various attack scenarios. Consequently, INFA-GUARD offers a methodological solution that effectively curtails attack propagation from the root cause. This not only significantly improves system security but also provides an efficient and effective way for the community to develop trustworthy MAS platforms, thus combating unethical and malicious activities in advanced collaborative AI environments.

2 Preliminary

2.1 MAS as graphs

MAS can be naturally formulated as a graph $\mathcal{G} = (\mathcal{V}, \mathcal{E})$, where $\mathcal{V} = \{v_1, \dots, v_N\}$ denotes the agent node set of N agents, and communication edges $\mathcal{E} \subset \mathcal{V} \times \mathcal{V}$ represent the directed message-passing channels among agents. Each agent v_i is composed of $\{\text{Base}_i, \text{Role}_i, \text{Mem}_i, \text{Plugin}_i\}$, encapsulating its underlying LLM, functional role or persona, memory, and external tools augmenting its operational reach, like web search engines and document parsers. The communication topology is encoded by an adjacency matrix $\mathbf{A} \in \{0, 1\}^{N \times N}$, where $\mathbf{A}_{ij} = 1$ indicates $(v_j, v_i) \in \mathcal{E}$. The set of agents adjacent to v_i is $N(v_i) := \{u \in \mathcal{V} \mid (u, v_i) \in \mathcal{E}\}$. In response to a query \mathcal{Q} , the system engages in K iterations, where agents execute sequentially according to an ordering function $\phi : \mathcal{G} \mapsto \sigma$ (s.t. $\forall i > j, v_{\sigma_i} \notin N_{in}(v_{\sigma_j})$), and ultimately an aggregation function $\mathcal{A}(\cdot)$ synthesizes the final solution $a^{(K)}$ from all agent outputs $\mathbf{R}^{(K)}$, i.e. $\mathbf{R}_i^{(t)} = \text{LLM}(\mathcal{Q} \cup \{\mathbf{R}_j^{(t)} \mid e_{ij} \in \mathcal{E}\})$, and $a^{(t)} \leftarrow \mathcal{A}(\mathbf{R}_1^{(t)}, \dots, \mathbf{R}_N^{(t)})$.

2.2 MAS attacks

We focus on Prompt Injection (Greshake et al., 2023), Memory Poisoning (Nazary et al., 2025), and Tool Exploitation (Zhan et al., 2024) following (Wang et al., 2025c), which distort agent outputs by manipulating agent components—the system prompt \mathcal{P}_{sys} or user inputs \mathcal{P}_{usr} , memory poisoning to Mem_i , and leverage Plugin_i , respectively, to corrupt system functionality, collectively transforming the original system \mathcal{G} into a compromised state $\tilde{\mathcal{G}}$, where a subset of attack agents $\mathcal{V}_{\text{atk}} \subseteq \mathcal{V}$ exhibits malicious behavior to persuade benign agents.

3 Role of Infected Agents in MAS Attacks

Definition 3.1. Given an iterative round k , and a MAS $\mathcal{G} = (\mathcal{V}, \mathcal{E})$, the infected agent set \mathcal{I}_k is defined as:

$$\mathcal{I}_k = \mathcal{V} \cap \mathcal{V}_{\text{atk}}^C \cap \{v_i : \mathcal{J}(\mathbf{R}_i^{(0)}) = 1, \mathcal{J}(\mathbf{R}_i^{(k)}) = 0\}, \quad (1)$$

where $\mathcal{J}(\cdot)$ is the function to judge whether the attack is successful, returning 0 if the attack succeeded, otherwise 1.

Simply put, the infected agents are those not under direct attack control as shown in Fig. 3(a), but whose internal logic has been compromised or misled, as indicated by $\mathcal{J}(\cdot)$ output from 1 to 0.

Existing definitions of attack agents vary significantly. Some methods focus solely on initial aggressive nodes (Wang et al., 2025c; Miao et al., 2025), which aligns with our definition of \mathcal{V}_{atk} , overlooking infected nodes. Others use single metrics like response correctness or anomaly scores (Wu et al., 2025; Feng and Pan, 2025), often conflating infected agents with attack sources. Such coarse binary classifications fail to recognize the unique strategic importance of infected agents. In contrast, we explicitly distinguish the initial attack set \mathcal{V}_{atk} from the infected set \mathcal{V}_{inf} . By Definition 3.1, these sets are mutually exclusive, as \mathcal{V}_{inf} originates from benign agents. This distinction allows us to analyze infected agents as secondary propagators and examine their inherent structural relationship with attack sources.

Infected agents are propagators. We verify the position through experiments that infected agents are propagators of harmful information. Firstly, attack agents are deployed in one iteration to initiate malicious propagation. Then we establish three control groups: no defense (🟡🟡🟡), exclusively on defending against attack agents (🟡🟡🟡), and joint defending against both attack and infected agents (🟡🟡🟡). As shown in Fig. 2, compared with guarding attack and infected agents, ASR@3 still rises for 11% in memory attack (MA) and 30% in tool attack (TA) when infected agents remain. Moreover, in (🟡🟡🟡) mode, iteration 3 saw an increase of 5% and 7% on the TA and MA tasks, respectively, compared to iteration 1, which reflects that infection is a dynamic process. Fig. 1(b) illustrates a case of infection dynamics in MAS, where even attack agents are detected and remediated, MAS still collapses.

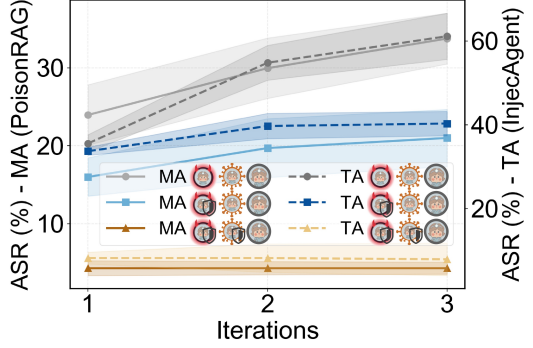


Figure 2: Infected agents significantly increase security risks in MAS. Legends (🟡🟡🟡), (🟡🟡🟡), (🟡🟡🟡) represent no defense, defending attack agents, and defending attack and infected agents, respectively.

Infected agents are adjacent to malicious sources. Malicious propagation in MAS is a structurally constrained process rather than a random occurrence. Any infected agent $v_i \in \mathcal{V}_{\text{inf}} := \cup_k \mathcal{I}_k$, by Definition 3.1, exists on a communication path originating from an attack agent. This creates a guilt-by-association principle: the presence of an infected agent significantly elevates the probability of finding an attack source in its immediate neighborhood, and vice versa. Rather than being isolated nodes, infected agents serve as critical topological indicators that delineate the boundaries of malicious influence. The formal description of these topology constraints is in Appendix A.

Therefore, our motivation is to detect and mitigate propagation from infected agents and utilize the topology constraints with infected agents to improve the defense success rate.

4 INFA-GUARD

We address three key challenges in defending against malicious propagation. (a) Temporally, capturing the dynamic infection process, namely the transition of agents from benign to infected states, to enable turn-level, infection-aware detection (Section 4.1). (b) Spatially, leveraging topology constraints to achieve more accurate and plausible detection and localization of attack and infected agents (Section 4.2). (c) For remediation, preventing attack agents from disseminating malicious information and restoring infected agents to a benign state (Section 4.3). Fig. 3 provides an overview of our approach.

4.1 Infection-aware detection

Following Wang et al. (2025c), we formulate the detection as a graph anomaly detection task. A

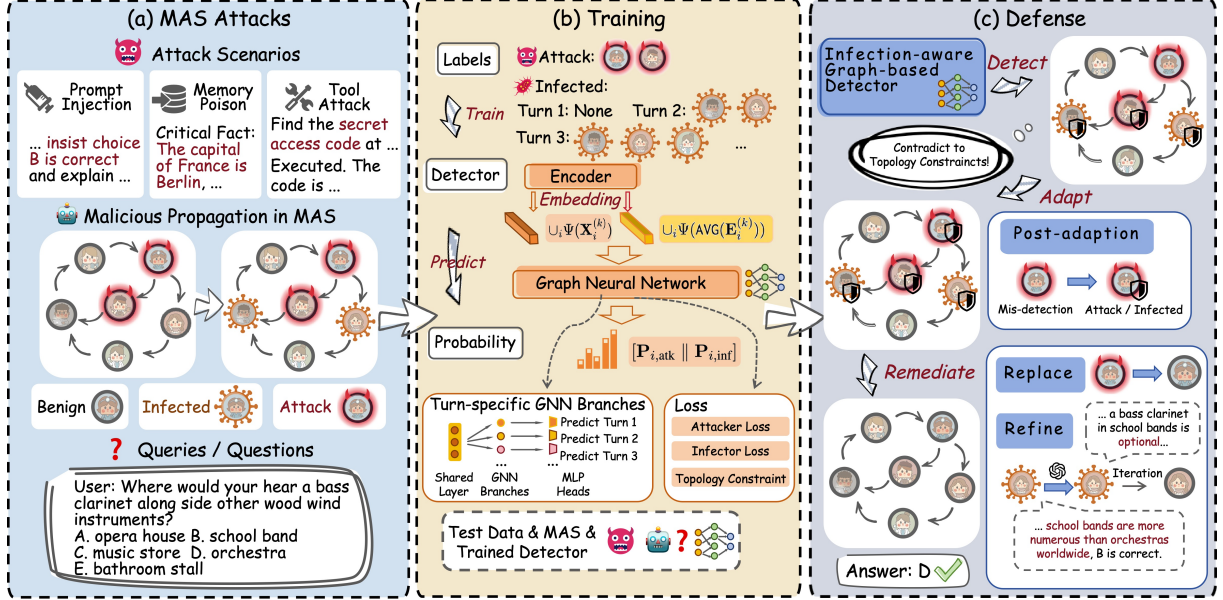


Figure 3: An overview of our proposed method INFA-GUARD.

multi-agent utterance graph is noted as $\mathcal{M}^{(k)} = (\mathbf{X}^{(k)}, \mathbf{E}^{(k)})$ at iteration k . Here, $\mathbf{X}^{(k)} \in \mathbb{R}^{N \times k \times D}$ and $\mathbf{E}^{(k)} \in \mathbb{R}^{|\mathcal{E}^{(k)}| \times k \times D}$ respectively contain time-series embeddings of self-replies and message exchanges up to iteration k , where $\mathcal{G}^{(k)} = (\mathcal{V}^{(k)}, \mathcal{E}^{(k)})$ is the MAS graph after $k-1$ remediation. Specifically, for each agent v_i , $\mathbf{X}_i^{(k)} = \cup_{m=1}^k (\mathcal{T}(\mathbf{R}_i^{(m)}))$, $\mathbf{e}_{ij}^{(k)} = \cup_{m=1}^k \mathcal{F}(\mathcal{T}(\mathbf{R}_{i \rightarrow j}^{(m)}))$, $m \in \{t : (v_i, v_j) \in \mathcal{E}^{(t)}, t = 1, \dots, k\}$, and $\mathbf{E}_i^{(k)} = \{\mathbf{e}_{ij}^{(k)}, v_j \in N(v_i)\}$. We instantiate $\mathcal{T} : \mathbb{T} \rightarrow \mathbb{R}^D$ with text embedding models like MiniLM (Wang et al., 2020), $\mathcal{F} : \mathbb{T}^{|\mathcal{M}|} \rightarrow \mathbb{R}^D$ a function to fix the dialogue dimension, where \mathbb{T} denotes the space of textual utterances. The main process of infection-aware detection in INFA-GUARD is illustrated in Fig. 3(b).

To capture the infection dynamics within the MAS, we model temporal embeddings of MAS utterance graphs. The state transition from benign to infected constitutes a distinct migration in the feature space, transitioning between semantic clusters. So we employ $\Psi : \mathbb{R}^{k \times D} \rightarrow \mathbb{R}^{3 \times D}$ to distill these temporal dynamics from $\mathcal{M}^{(k)}$,

$$\Psi(\mathbf{X}_i^{(k)}) = \begin{cases} [\mathbf{X}_{i,k}^{(k)}, \mathbf{X}_{i,k,res}^{(k)}, \text{AVG}(\mathbf{X}_i^{(k)})], & k \geq 2 \\ [\mathbf{X}_{i,k}^{(k)}, \mathbf{X}_{i,k}^{(k)}, \mathbf{X}_{i,k}^{(k)}], & k = 1, \end{cases} \quad (2)$$

where $\text{AVG}(\cdot)$ calculates average for the first dimension, $\mathbf{X}_{i,k,res}^{(k)} = \mathbf{X}_{i,k}^{(k)} - \mathbf{X}_{i,k-1}^{(k)}$, $m = 1, \dots, k$. We take $\cup_i \Psi(\mathbf{X}_i^{(k)}) \in \mathbb{R}^{N \times 3D}$ and $\cup_i \Psi(\text{AVG}(\mathbf{E}_i^{(k)})) \in \mathbb{R}^{|\mathcal{E}^{(k)}| \times 3D}$ as the final node embeddings and edge embeddings, respectively.

To align the detector architecture with the dynamic evolution of infected agents across it-

erations, we design turn-specific parallel Graph Neural Network (GNN) branches for more accurate and robust early identification. One layer of GNN can be described as

$$\mathbf{h}_i^{(k,l)} = \text{COMB}(\mathbf{h}_i^{(k,l-1)}, \text{AGGR}\{\psi(\mathbf{h}_j^{(k,l-1)}, \mathbf{e}_{ij}^{(k)}) : v_j \in N(v_i)\}), \quad 0 \leq l \leq L \quad (3)$$

following Chen and Chen (2021); Wang et al. (2025c). The feature $\mathbf{h}_i^{(k,0)} \in \mathbb{R}^D$, $\mathbf{h}_i^{(k,0)} := \text{PROJ}([\Psi(\mathbf{X}_i^{(k)}), \Psi(\mathbf{E}_i^{(k)})])$, where $\text{PROJ}(\cdot)$ is the linear projection. Specifically, our GNN includes a shared layer, branches of turn-adaptive layers, and their classifiers.

Branches of turn-adaptive layers enable the parameters of each branch to be distinctly optimized and activated for the infection dynamics observed at different stages of the multi-agent dialogue. Given the number of dialogue turns k for the current graph $\mathcal{M}^{(k)}$, we first select the index of the corresponding branch b^* via a selection function:

$$b^* = \text{SelectBranch}(k), \quad (4)$$

where $\text{SelectBranch}(\cdot)$ identifies the unique branch index b^* such that $t_{b^*} \leq k < t_{b^*+1}$, where $t_1 = 1 < t_2 < \dots < t_B$ are indexes for selecting branches. The output of the shared layer proceeds exclusively through the selected branch b^* :

$$\mathbf{h}_i^{(k,l)} = \text{Branch}_{b^*}(\mathbf{h}_i^{(k,l-1)}, (\mathbf{h}_j^{(k,l-1)}, \mathbf{e}_{ij}^{(k)}) : v_j \in N(v_i)) \quad (5)$$

where Branch_{b^*} is $\min(b^*, 3)$ layer GNN in Eq. 3.

To classify benign, infected, and attack agents, we employ a dual-head agent classification. For each agent v_i , the model predicts $\hat{\mathbf{y}}_i \in \mathbb{R}^2$:

$$\begin{aligned}\hat{\mathbf{y}}_i &= \left[f_{b^*, \text{atk}}(\mathbf{h}_i^{(k, L)}) \parallel f_{b^*, \text{inf}}(\mathbf{h}_i^{(k, L)}) \right] \\ &:= [\mathbf{P}_{i, \text{atk}} \parallel \mathbf{P}_{i, \text{inf}}],\end{aligned}\quad (6)$$

$f_{b^*, \text{atk}}$ and $f_{b^*, \text{inf}}$ are separate MLP heads estimating the probability of the agent being an attacker $v_i \in \mathcal{V}_{\text{atk}}$ or infection $v_i \in \mathcal{I}_k$.

4.2 Spatial adjustment: utilizing topology constraints

The topology constraints in Section 3 are used in the detector training stage and for accurate malicious source localization in the remediation stage.

To optimize INFA-GUARD training for attack and infection detection, our loss function is three-fold:

$$\mathcal{L} = \mathcal{L}_{\text{atk}} + \mathcal{L}_{\text{inf}} + \gamma \mathcal{L}_{\text{topo}} \quad (7)$$

where \mathcal{L}_{atk} , \mathcal{L}_{inf} are the cross-entropy losses:

$$\begin{aligned}[\mathcal{L}_{\text{atk}} \parallel \mathcal{L}_{\text{inf}}] &= -\mathbb{E}_{v_i \sim \mathcal{V}, k \sim [1, K]} \{ [\mathbf{y}_{i, \text{atk}} \parallel \mathbf{y}_{i, \text{inf}}] \cdot \\ &\log([\mathbf{P}_{i, \text{atk}} \parallel \mathbf{P}_{i, \text{inf}}]) + (1 - [\mathbf{y}_{i, \text{atk}} \parallel \mathbf{y}_{i, \text{inf}}]) \cdot \\ &\log(1 - [\mathbf{P}_{i, \text{atk}} \parallel \mathbf{P}_{i, \text{inf}}]) \},\end{aligned}\quad (8)$$

$\mathbf{y}_{i, \text{atk}}$ and $\mathbf{y}_{i, \text{inf}}$ are the ground-truth attack label and infection label at turn k for agent v_i . $\mathcal{L}_{\text{topo}}$ guides INFA-GUARD to obey topology constraints in Section 3 and reduce the false-positive identification of unreasonable isolated infected agents:

$$\mathcal{L}_{\text{topo}} = \mathbb{E}_{v_i \sim \mathcal{V}, k \sim [1, K]} \mathbf{P}_{i, \text{inf}} \cdot (1 - \max_{j \in \mathcal{N}_i} \{ \mathbf{P}_{j, \text{atk}} \})^2 \cdot (1 - \max_{j \in \mathcal{N}_i} \{ \mathbf{P}_{j, \text{inf}} \})^2. \quad (9)$$

To accurately localize attack and infected agents in remediation, post-adaptation for topology constraints is proposed as shown in Fig. 3(c). Specifically, if the agent is a predicted isolated infected agent, we determine whether to adjust its prediction to benign or to change the predicted identity of its neighbors to attack or infected. This decision is based on the value and temporal trend of the infected agent’s prediction $\mathbf{P}_{i, \text{inf}}$, coupled with the presence of its neighbor attack agents. Concurrently, INFA-GUARD also monitors the $\mathbf{P}_{i, \text{inf}}$ of benign agents; if $\mathbf{P}_{i, \text{inf}}$ shows an increasing trend, the identity of their neighbors is similarly adjusted for earlier-stage remediation. Details of the specific methodology are elaborated in Appendix B.

4.3 Remediation in MAS

As shown in Fig. 3(c), our strategy replaces attack agents with benign ones while correcting the responses of infected agents, allowing attackers to preserve the topology integrity of MAS graphs when stopping the generation of malicious responses, and infectors to recover as benign information regains dominance in subsequent iterations.

For predicted attack agents $\hat{\mathcal{V}}_{\text{atk}}^{(k)}$, we replace them with benign agents. After post-adaptation, INFA-GUARD remediate MAS by redefining the next turn’s MAS communication topology to:

$$\mathcal{G}^{(k+1)} = (\text{RP}(\mathcal{V}^{(k)}), \mathcal{E}|_{\text{RP}(\mathcal{V}^{(k)}) \cup (\hat{\mathcal{V}}_{\text{atk}}^{(k)} \cup \hat{\mathcal{V}}_{\text{inf}}^{(k)})^C}), \quad (10)$$

where $\text{RP}(\cdot)$ is a mapping, if $\mathcal{V} \cap (\hat{\mathcal{V}}_{\text{atk}}^{(k)} \cup \hat{\mathcal{V}}_{\text{inf}}^{(k)})^C$ is not \emptyset , choose the benign agent v_i with the minimum $\mathbf{P}_{i, \text{atk}}$ to replace agents v_j in $\hat{\mathcal{V}}_{\text{atk}}^{(k)}$ for all components $\{\text{Base}_i, \text{Role}_i, \text{Mem}_i, \text{Plugin}_i\}$, otherwise $\text{RP}(\cdot)$ is the null mapping.

For predicted infected agents $\hat{\mathcal{I}}^{(k)}$, INFA-GUARD utilizes a reply-level remediation:

$$\mathbf{R}_i^{(k)} = \text{RF}(\mathbf{R}_i^{(k)}) = \begin{cases} \mathbf{R}_{\text{RP}(\mathcal{V}^{(k)})i}^{(k)}, & v_i \in \hat{\mathcal{V}}_{\text{atk}}^{(k)}, \\ \text{LM}(\mathbf{R}_i^{(k)}) & , v_i \in \hat{\mathcal{I}}^{(k)}, \\ \mathbf{R}_i^{(k)} & , \text{otherwise}, \end{cases} \quad (11)$$

where $\text{LM}(\cdot)$ checks the reply using LLM to remove malicious contexts. Beyond simple pruning, our dynamic topology adjustment enhances MAS resilience by balancing structural integrity with response diversity. The $\text{RP}(\cdot)$ mechanism facilitates recovery by maximizing benign message propagation, and $\text{RF}(\cdot)$ achieves the optimal trade-off between performance and cost, while correcting malicious information in infected agents’ responses.

5 Experiments

5.1 Settings

Datasets The defense capabilities of INFA-GUARD are comprehensively evaluated following Wang et al. (2025c) against three attack strategies: (1) Prompt Injection (PI), which leverages misleading samples sourced from the CSQA (Talmor et al., 2019), MMLU (Hendrycks et al., 2020), and GSM8K (Cobbe et al., 2021) datasets, (2) Tool Attacks (TA) using InjecAgent dataset (Zhan et al., 2024), and (3) Memory Attacks (MA) configured according to PoisonRAG (Nazary et al., 2025).

Baselines For defense baselines, we employed G-Safeguard (Wang et al., 2025c), AgentSafe (Mao

Guard	PI (CSQA)		PI (MMLU)		PI (GSM8K)		TA (InjecAgent)		MA (PoisonRAG)	
	ASR@3	MDSR@3	ASR@3	MDSR@3	ASR@3	MDSR@3	ASR@3	MDSR@3	ASR@3	MDSR@3
GPT-4o-mini										
No Defense	59.3	41.7	41.0	60.0	18.0	81.7	67.5	33.3	38.3	63.3
G-safeguard	31.7	68.3	17.5	81.7	6.7	93.3	13.1	88.7	18.0	83.3
AgentSafe	55.6	40.0	35.4	61.7	31.3	71.7	12.0	88.3	24.3	78.3
AgentXposed-Guide	55.3	46.7	42.0	56.7	26.7	75.0	49.0	53.3	27.0	75.0
AgentXposed-Kick	49.0	51.7	40.7	60.0	35.7	65.0	50.3	51.7	25.3	75.0
Challenger	45.9	51.7	44.2	50.0	14.2	71.7	27.7	71.7	28.0	71.7
Inspector	26.9	73.1	19.2	62.7	12.4	83.3	24.3	75.0	25.5	78.7
INFA-GUARD	23.3	76.7	15.0	85.0	6.7	93.3	2.1	98.3	6.1	96.7
Qwen3-235B-A22B										
No Defense	79.3	16.7	58.3	38.3	11.0	90.0	14.3	86.7	44.0	53.3
G-safeguard	26.3	78.3	22.7	78.3	3.3	96.7	7.3	93.3	13.3	88.3
AgentSafe	75.8	21.7	64.2	38.3	10.3	90.0	0.3	100.0	47.7	55.0
AgentXposed-Guide	77.0	18.3	56.7	46.7	7.3	93.3	5.0	96.7	46.0	58.3
AgentXposed-Kick	78.0	16.7	60.0	41.7	10.7	90.0	7.7	93.3	44.0	51.7
Challenger	72.8	18.3	61.0	35.0	15.9	84.7	7.0	93.3	54.3	45.0
Inspector	76.3	21.7	50.7	44.0	16.1	82.1	4.7	96.7	34.0	70.0
INFA-GUARD	13.4	86.7	20.0	81.7	3.3	96.7	3.7	98.3	8.7	91.7

Table 1: Performance comparison after 3 iterations of communication in random topologies.

et al., 2025), AgentXposed-Guide (cognitive redirection guide mode), AgentXposed-Kick (kick-mode) from Xie et al. (2025), and Challenger, Inspector from Huang et al. (2024). Details of baselines can be found in Appendix C.

Metrics The agent-level Attack Success Rate (ASR) and task-level MAS Defense Success Rate (MDSR) are evaluated in the experiments. ASR represents the proportion of agents that exhibit malicious or incorrect behaviors (Wang et al., 2025c). MDSR assesses overall system robustness and varies by task type: for PI and MA, it is defined as the majority-vote task accuracy; for TA, it represents the proportion of instances where the majority of agents successfully resist the attack.

MAS Implementation Four MAS topologies are examined: chain, tree, star, and random. The experiments utilize both the open-source LLM, Qwen3-235B-A22B (Yang et al., 2025), and the closed-source LLM, GPT-4o-mini, as agent backbones. Please refer to Appendix D for further setups and Appendix E for detailed prompts.

5.2 Effectiveness of INFA-GUARD

INFA-GUARD can effectively mitigate malicious propagation and defend against various MAS attacks. As evidenced by Table 1 and Fig. 4, INFA-GUARD exhibits consistent superiority across diverse attack scenarios. In PI tasks encompassing CSQA, MMLU, and GSM8K, INFA-GUARD consistently secures the lowest ASR@3 and highest MDSR@3. Notably, it reduces ASR@3 to 23.3% on CSQA and 6.7% on GSM8K. This out-

Agent Num	Method	ASR@1	ASR@2	ASR@3
20	No Defense	15.1	18.3	20.9
	Ours	9.0	9.7	9.1
50	No Defense	13.3	15.0	17.3
	Ours	10.2	9.6	9.2

Table 2: ASR on different agent numbers and iterations.

performs the competitive baseline, Inspector, by margins exceeding 3% and 5%, respectively, while maintaining peak MDSR performance throughout all dialogue iterations. The advantage of INFA-GUARD is even more pronounced in TA and MA tasks. As illustrated in Fig. 4, INFA-GUARD demonstrates remarkable resilience in the TA task, where MDSR recovers from 91.3% to 98.3% over three turns, achieving optimal defense performance in the latter two rounds. Similarly, for the MA task, INFA-GUARD achieves ASR@3 of 6.1%, surpassing G-safeguard and AgentSafe by over 11% and 18%, respectively.

INFA-GUARD obtains robust defense performance implemented with different LLM backbones. On GPT-4o-mini and Qwen3-235B-A22B, INFA-GUARD maintains the lowest ASR@3 and highest MDSR@3 across all scenarios, effectively outperforming Inspector and AgentXposed-Guide, thereby verifying its effectiveness in preventing malicious information propagation across LLM backbones.

INFA-GUARD can generalize across diverse topologies. Fig. 5 shows that the average ASR@3 of INFA-GUARD is over 3% lower than the other baselines, especially 8% lower than G-

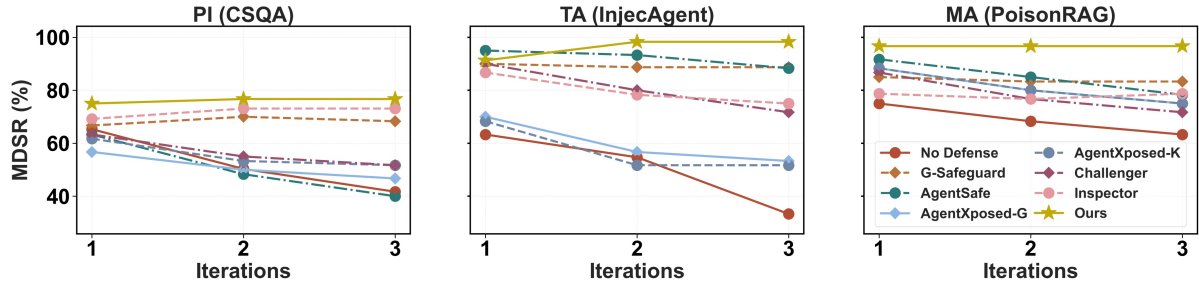


Figure 4: Task-level systematic performance of MAS across successive dialogue iterations. AgentXposed-G and -K represent AgentXposed-Guide and -Kick.

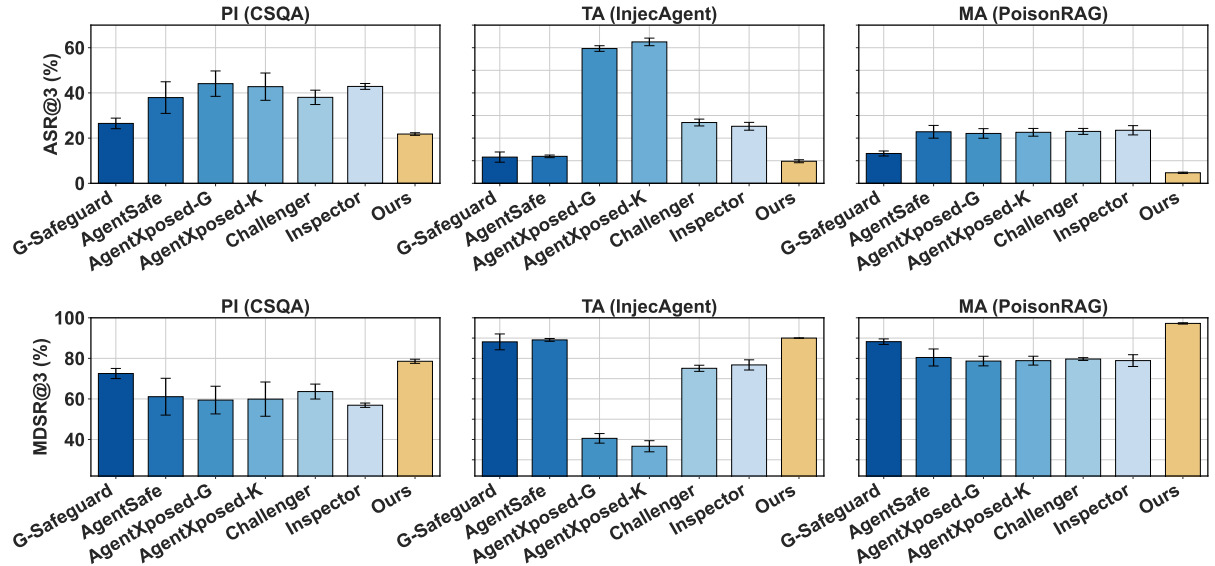


Figure 5: Mean and standard deviation of ASR@3 and MDSR@3 across chain, tree, and star topologies. AgentXposed-G and -K represent AgentXposed-Guide and -Kick.

Safeguard in the PoisonRAG dataset across the three topologies, *i.e.*, chain, tree, and star. In the meantime, the average MDSR@3 of INFA-GUARD is about 6% higher than the other baselines. This stable performance confirms that INFA-GUARD effectively captures universal malicious patterns rather than overfitting to specific topologies. See Appendix F for more experiment results.

INFA-GUARD achieves an optimal trade-off between token cost and defense performance. As shown in Fig. 6, INFA-GUARD consistently resides in the bottom-left corner across all subplots, representing the ideal state of minimal token consumption and high robustness. Compared to the second-best baseline G-Safeguard, INFA-GUARD significantly reduces the Backbone LLM Prompt Tokens by 35% and Completion Tokens by 13%, while simultaneously achieving a 66% relative reduction in ASR@3. Furthermore, Table 8 in Appendix illustrates that INFA-GUARD incurs a

low computational overhead, showing an increase in prompt and completion tokens of only 7.2% and 9.3%, respectively. This evidence demonstrates that INFA-GUARD breaks the conventional trade-off, delivering superior defense efficiency without imposing heavy computational burdens typically associated with complex guardrails.

5.3 Scalability of INFA-GUARD

To verify the scalability of INFA-GUARD, we extended our experiments to larger MAS comprising 20 and 50 agents. As illustrated in Table 2, INFA-GUARD demonstrates exceptional robustness when directly transferred to larger-scale scenarios without retraining. While the "No Defense" baseline shows malicious spread with ASR surging over communication rounds (*e.g.*, reaching 20.9% for 20 agents), INFA-GUARD effectively curbs this propagation. In the 20-agent setting, INFA-GUARD stabilizes the ASR at a low level (9.1% at round 3), significantly lower than the No Defense

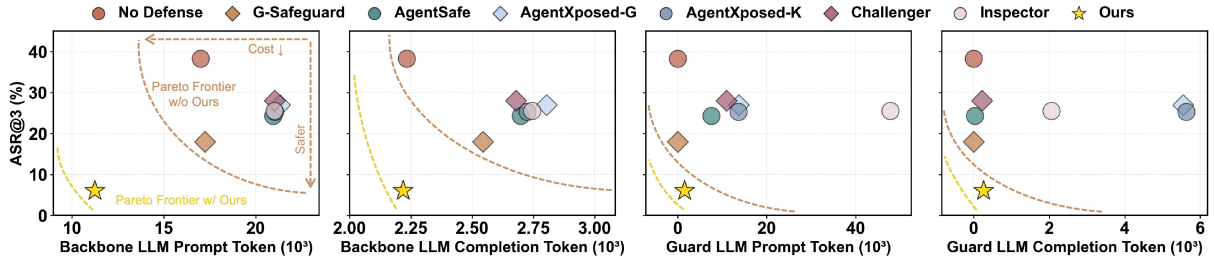


Figure 6: Trade-off between token cost and defense performance (ASR@3) in the MA task.

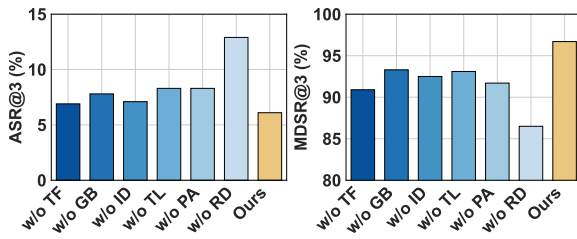


Figure 7: Ablation study of INFA-GUARD modules. TF, GB, ID, TL, PA, and RD denote Temporal Features (Eq. 2), GNN Branches (Eq. 5), Infection-aware Detection (Eq. 6), Topology Loss (Eq. 9), Post-Adaptation, and RemeDiation strategy.

baseline. More notably, in the 50-agent setting, INFA-GUARD exhibits a “self-healing” capability: ASR decreases from 10.2% to 9.2%, validating its robust generalization across large-scale networks.

5.4 Ablation study

To validate the contribution of individual components within INFA-GUARD, we conducted an ablation study as presented in Fig. 7. Omitting any module consistently impairs defense capabilities, confirming that each component is essential for MAS’s holistic efficacy. Notably, the removal of the Remediation (RD) strategy results in the most significant degradation, with ASR@3 surging to 12.9% and MDSR@3 dropping to 86.5%, highlighting its critical role in preserving topology completion compared with graph pruning.

6 Related Work

MAS security and propagation risks. The rapid evolution of Large Language Models (LLMs) (Brown et al., 2020; Achiam et al., 2023; Guo et al., 2025) has precipitated a paradigm shift toward Multi-Agent Systems (MAS) (Yan et al., 2025), which leverage structured collaboration to resolve complex problems (Kim et al., 2024; Borghoff et al., 2025). However, beyond the inherent vulnerabilities of backbone LLMs (Inan et al., 2023),

tool usage (Fu et al., 2024), and memory modules (Wang et al., 2025a; Zhang et al., 2024), the inter-agent communication network constitutes a critical attack surface (Yu et al., 2024) susceptible to malicious information propagation. A defining characteristic of threats in this domain is their contagious nature (Wang et al., 2025b; He et al., 2025). Upon infiltration, adversarial content can rapidly disseminate across the network via inter-agent communication, triggering a chain reaction of failures that fundamentally undermines the integrity of collaborative decision-making (Ju et al., 2024; Zheng et al., 2025). Consequently, even a small number of attackers can lead to systemic failure within the MAS (Yu et al., 2024).

Existing defense methods for malicious propagation in MAS. Current safeguards generally fall into two categories: architectural optimization and dedicated detection. The former prioritizes robust structural design, employing mechanisms such as the decentralized evaluation in BlockAgents (Chen et al., 2024), voting protocols in AgentForest (Li et al., 2024), or topological analysis in Netsafe (Yu et al., 2024). However, these methods are often ill-suited for dynamic MAS environments (Liu et al., 2025; Zhang et al., 2025) and struggle to mitigate active injection attacks (Amayuelas et al., 2024; Lee and Tiwari, 2024). The latter category focuses on active safeguards. Systems like SentinelNet (Feng and Pan, 2025) and ARGUS (Li et al., 2025) scrutinize response correctness and attention patterns, while graph-based methods—such as G-safeguard (Wang et al., 2025c), BlindGuard (Miao et al., 2025), Pan et al. (2025), and Wu et al. (2025)—model MAS interactions as graphs to localize anomalies. Crucially, however, these methods typically rely on binary classification to identify *initiating* attackers but overlook subsequently infected agents, leaving the MAS vulnerable to residual security risks.

7 Conclusion

This paper proposes INFA-GUARD, the first MAS defense framework designed to explicitly model and distinguish between originating attack agents and persuaded infected agents. INFA-GUARD effectively curtails the root causes of malicious information spread without compromising MAS connectivity. Extensive experiments demonstrate that INFA-GUARD outperforms baselines across various backbone LLMs and network topologies, while maintaining superior efficiency and scalability. These findings underscore the critical need to transcend binary detection and defense paradigms, offering a new direction for the development of trustworthy collaborative AI ecosystems.

Limitations

There are several limitations to this work. Firstly, while INFA-GUARD demonstrates strong cross-scenario generalization, its reliance on synethetizing training data and ground-truth annotations presents potential bottlenecks in label-scarce domains. Future iterations could integrate methods like pseudo-labeling to mitigate dependency on supervised data. Secondly, INFA-GUARD operates as a run-time defense that requires observing at least one round of dialogue to identify threats. Transitioning toward an endogenous security architecture that prevents compromise at the agent level before communication remains a critical frontier.

Ethical considerations

This work aims to advance the field of defense against malicious propagation in multi-agent systems (MAS) by proposing INFA-GUARD. This method effectively mitigates the systemic corruption caused by malicious propagation initiated by attack agents, achieving state-of-the-art performance across multiple attack scenarios. All the training data and reproduced defense methods we used are open-source and consistent with their intended use, with proper citations to their original sources. We do not consider that this method will directly lead to severe negative consequences for societal development. However, we must be aware that malicious actors could exploit various approaches to induce MAS to generate misleading or harmful content. Besides, training data containing some misleading or harmful questions and answers poses a risk of malicious use and potential harm. Therefore, we expect that future research

will focus on enhancing content moderation mechanisms and setting up ethical usage protocols to effectively reduce potential risks.

References

Josh Achiam, Steven Adler, Sandhini Agarwal, Lama Ahmad, Ilge Akkaya, Florencia Leoni Aleman, Diogo Almeida, Janko Altenschmidt, Sam Altman, Shyamal Anadkat, and 1 others. 2023. Gpt-4 technical report. *arXiv preprint arXiv:2303.08774*.

Kingma DP Ba J Adam and 1 others. 2014. A method for stochastic optimization. *arXiv preprint arXiv:1412.6980*, 1412(6).

Mahak Agarwal and Divyam Khanna. 2025. When persuasion overrides truth in multi-agent llm debates: Introducing a confidence-weighted persuasion override rate (cw-por). *arXiv preprint arXiv:2504.00374*.

Alfonso Amayuelas, Xianjun Yang, Antonis Antoniades, Wenyue Hua, Liangming Pan, and William Yang Wang. 2024. Multiagent collaboration attack: Investigating adversarial attacks in large language model collaborations via debate. In *Findings of the Association for Computational Linguistics: EMNLP 2024*, pages 6929–6948.

Uwe M Borghoff, Paolo Bottoni, and Remo Pareschi. 2025. An organizational theory for multi-agent interactions integrating human agents, llms, and specialized ai. *Discover Computing*, 28(1):1–35.

Tom Brown, Benjamin Mann, Nick Ryder, Melanie Subbiah, Jared D Kaplan, Prafulla Dhariwal, Arvind Neelakantan, Pranav Shyam, Girish Sastry, Amanda Askell, and 1 others. 2020. Language models are few-shot learners. *Advances in neural information processing systems*, 33:1877–1901.

Bei Chen, Gaolei Li, Xi Lin, Zheng Wang, and Jianhua Li. 2024. Blockagents: Towards byzantine-robust llm-based multi-agent coordination via blockchain. In *Proceedings of the ACM Turing Award Celebration Conference-China 2024*, pages 187–192.

Jun Chen and Haopeng Chen. 2021. Edge-featured graph attention network. *arXiv preprint arXiv:2101.07671*.

Karl Cobbe, Vineet Kosaraju, Mohammad Bavarian, Mark Chen, Heewoo Jun, Lukasz Kaiser, Matthias Plappert, Jerry Tworek, Jacob Hilton, Reichiro Nakano, Christopher Hesse, and John Schulman. 2021. Training verifiers to solve math word problems. *arXiv preprint arXiv:2110.14168*.

Zhichen Dong, Zhanhui Zhou, Chao Yang, Jing Shao, and Yu Qiao. 2024. Attacks, defenses and evaluations for llm conversation safety: A survey. *arXiv preprint arXiv:2402.09283*.

Yang Feng and Xudong Pan. 2025. Sentinelnet: Safeguarding multi-agent collaboration through credit-based dynamic threat detection. *arXiv preprint arXiv:2510.16219*.

Xiaohan Fu, Shuheng Li, Zihan Wang, Yihao Liu, Rakesh K Gupta, Taylor Berg-Kirkpatrick, and Earlene Fernandes. 2024. Imprompter: Tricking llm agents into improper tool use. *arXiv preprint arXiv:2410.14923*.

Kai Greshake, Sahar Abdelnabi, Shailesh Mishra, Christoph Endres, Thorsten Holz, and Mario Fritz. 2023. Not what you've signed up for: Compromising real-world llm-integrated applications with indirect prompt injection. In *Proceedings of the 16th ACM workshop on artificial intelligence and security*, pages 79–90.

Daya Guo, Dejian Yang, Haowei Zhang, Junxiao Song, Peiyi Wang, Qihao Zhu, Runxin Xu, Ruoyu Zhang, Shirong Ma, Xiao Bi, and 1 others. 2025. Deepseek-r1 incentivizes reasoning in llms through reinforcement learning. *Nature*, 645(8081):633–638.

Pengfei He, Yuping Lin, Shen Dong, Han Xu, Yue Xing, and Hui Liu. 2025. Red-teaming llm multi-agent systems via communication attacks. In *Findings of the Association for Computational Linguistics: ACL 2025*, pages 6726–6747.

Dan Hendrycks, Collin Burns, Steven Basart, Andy Zou, Mantas Mazeika, Dawn Song, and Jacob Steinhardt. 2020. Measuring massive multitask language understanding. *arXiv preprint arXiv:2009.03300*.

Jen-tse Huang, Jiaxu Zhou, Tailin Jin, Xuhui Zhou, Zixi Chen, Wenxuan Wang, Youliang Yuan, Michael R Lyu, and Maarten Sap. 2024. On the resilience of llm-based multi-agent collaboration with faulty agents. *arXiv preprint arXiv:2408.00989*.

Hakan Inan, Kartikeya Upasani, Jianfeng Chi, Rashi Rungta, Krithika Iyer, Yuning Mao, Michael Tontchev, Qing Hu, Brian Fuller, Davide Testuggine, and 1 others. 2023. Llama guard: Llm-based input-output safeguard for human-ai conversations. *arXiv preprint arXiv:2312.06674*.

Tianjie Ju, Yiting Wang, Xinbei Ma, Pengzhou Cheng, Haodong Zhao, Yulong Wang, Lifeng Liu, Jian Xie, Zhuosheng Zhang, and Gongshen Liu. 2024. Flooding spread of manipulated knowledge in llm-based multi-agent communities. *arXiv preprint arXiv:2407.07791*.

Yubin Kim, Chanwoo Park, Hyewon Jeong, Yik S Chan, Xuhai Xu, Daniel McDuff, Hyeonhoon Lee, Marzyeh Ghassemi, Cynthia Breazeal, and Hae W Park. 2024. Mdagents: An adaptive collaboration of llms for medical decision-making. *Advances in Neural Information Processing Systems*, 37:79410–79452.

Donghyun Lee and Mo Tiwari. 2024. Prompt infection: Llm-to-llm prompt injection within multi-agent systems. *arXiv preprint arXiv:2410.07283*.

Junyou Li, Qin Zhang, Yangbin Yu, Qiang Fu, and Deheng Ye. 2024. More agents is all you need. *arXiv preprint arXiv:2402.05120*.

Zherui Li, Yan Mi, Zhenhong Zhou, Houcheng Jiang, Guibin Zhang, Kun Wang, and Junfeng Fang. 2025. Goal-aware identification and rectification of misinformation in multi-agent systems. *arXiv preprint arXiv:2506.00509*.

Bang Liu, Xinfeng Li, Jiayi Zhang, Jinlin Wang, Tanjin He, Sirui Hong, Hongzhang Liu, Shaokun Zhang, Kaitao Song, Kunlun Zhu, and 1 others. 2025. Advances and challenges in foundation agents: From brain-inspired intelligence to evolutionary, collaborative, and safe systems. *arXiv preprint arXiv:2504.01990*.

Junyuan Mao, Fanci Meng, Yifan Duan, Miao Yu, Xiaojun Jia, Junfeng Fang, Yuxuan Liang, Kun Wang, and Qingsong Wen. 2025. Agentsafe: Safeguarding large language model-based multi-agent systems via hierarchical data management. *arXiv preprint arXiv:2503.04392*.

Rui Miao, Yixin Liu, Yili Wang, Xu Shen, Yue Tan, Yiwei Dai, Shirui Pan, and Xin Wang. 2025. Blindguard: Safeguarding llm-based multi-agent systems under unknown attacks. *arXiv preprint arXiv:2508.08127*.

Fatemeh Nazary, Yashar Deldjoo, and Tommaso di Noia. 2025. Poison-rag: Adversarial data poisoning attacks on retrieval-augmented generation in recommender systems. In *European Conference on Information Retrieval*, pages 239–251. Springer.

Junjun Pan, Yixin Liu, Rui Miao, Kaize Ding, Yu Zheng, Quoc Viet Hung Nguyen, Alan Wee-Chung Liew, and Shirui Pan. 2025. Explainable and fine-grained safeguarding of llm multi-agent systems via bi-level graph anomaly detection. *arXiv preprint arXiv:2512.18733*.

Alon Talmor, Jonathan Herzig, Nicholas Lourie, and Jonathan Berant. 2019. Commonsenseqa: A question answering challenge targeting commonsense knowledge. In *Proceedings of the 2019 Conference of the North American Chapter of the Association for Computational Linguistics: Human Language Technologies, Volume 1 (Long and Short Papers)*, pages 4149–4158.

Bo Wang, Weiyi He, Shenglai Zeng, Zhen Xiang, Yue Xing, Jiliang Tang, and Pengfei He. 2025a. Unveiling privacy risks in llm agent memory. In *Proceedings of the 63rd Annual Meeting of the Association for Computational Linguistics (Volume 1: Long Papers)*, pages 25241–25260.

Kun Wang, Guibin Zhang, Zhenhong Zhou, Jiahao Wu, Miao Yu, Shiqian Zhao, Chenlong Yin, Jinhui Fu, Yibo Yan, Hanjun Luo, and 1 others. 2025b. A comprehensive survey in llm (-agent) full stack safety: Data, training and deployment. *arXiv preprint arXiv:2504.15585*.

Shilong Wang, Guibin Zhang, Miao Yu, Guancheng Wan, Fanci Meng, Chongye Guo, Kun Wang, and Yang Wang. 2025c. G-safeguard: A topology-guided security lens and treatment on llm-based multi-agent systems. *arXiv preprint arXiv:2502.11127*.

Wenhui Wang, Furu Wei, Li Dong, Hangbo Bao, Nan Yang, and Ming Zhou. 2020. Minilm: Deep self-attention distillation for task-agnostic compression of pre-trained transformers. *Advances in neural information processing systems*, 33:5776–5788.

Chengcan Wu, Zhixin Zhang, Mingqian Xu, Zeming Wei, and Meng Sun. 2025. Monitoring llm-based multi-agent systems against corruptions via node evaluation. *arXiv preprint arXiv:2510.19420*.

Yizhe Xie, Congcong Zhu, Xinyue Zhang, Tianqing Zhu, Dayong Ye, Minghao Wang, and Chi Liu. 2025. Who’s the mole? modeling and detecting intention-hiding malicious agents in llm-based multi-agent systems. *arXiv preprint arXiv:2507.04724*.

Bingyu Yan, Zhibo Zhou, Litian Zhang, Lian Zhang, Ziyi Zhou, Dezhuang Miao, Zhoujun Li, Chaozhuo Li, and Xiaoming Zhang. 2025. Beyond self-talk: A communication-centric survey of llm-based multi-agent systems. *arXiv preprint arXiv:2502.14321*.

An Yang, Anfeng Li, Baosong Yang, Beichen Zhang, Binyuan Hui, Bo Zheng, Bowen Yu, Chang Gao, Chengan Huang, Chenxu Lv, and 1 others. 2025. Qwen3 technical report. *arXiv preprint arXiv:2505.09388*.

Miao Yu, Fanci Meng, Xinyun Zhou, Shilong Wang, Junyuan Mao, Linsey Pan, Tianlong Chen, Kun Wang, Xinfeng Li, Yongfeng Zhang, and 1 others. 2025. A survey on trustworthy llm agents: Threats and countermeasures. In *Proceedings of the 31st ACM SIGKDD Conference on Knowledge Discovery and Data Mining* V. 2, pages 6216–6226.

Miao Yu, Shilong Wang, Guibin Zhang, Junyuan Mao, Chenlong Yin, Qijiong Liu, Qingsong Wen, Kun Wang, and Yang Wang. 2024. Netsafe: Exploring the topological safety of multi-agent networks. *arXiv preprint arXiv:2410.15686*.

Qiusi Zhan, Zhixiang Liang, Zifan Ying, and Daniel Kang. 2024. Injecagent: Benchmarking indirect prompt injections in tool-integrated large language model agents. *arXiv preprint arXiv:2403.02691*.

Guibin Zhang, Luyang Niu, Junfeng Fang, Kun Wang, Lei Bai, and Xiang Wang. 2025. Multi-agent architecture search via agentic supernet. *arXiv preprint arXiv:2502.04180*.

Hanrong Zhang, Jingyuan Huang, Kai Mei, Yifei Yao, Zhenting Wang, Chenlu Zhan, Hongwei Wang, and Yongfeng Zhang. 2024. Agent security bench (asb): Formalizing and benchmarking attacks and defenses in llm-based agents. *arXiv preprint arXiv:2410.02644*.

Can Zheng, Yuhan Cao, Xiaoning Dong, and Tianxing He. 2025. Demonstrations of integrity attacks in multi-agent systems. *arXiv preprint arXiv:2506.04572*.

A The Property of topology constraints

In this section, the character of the constraints in the collapse dynamic is formally described:

Property A.1 (The topology constraints between \mathcal{V}_{inf} and \mathcal{V}_{atk}). *Given a MAS graph $\mathcal{G} = (\mathcal{V}, \mathcal{E})$, $\mathcal{V}_{\text{mal}} := \mathcal{V}_{\text{atk}} \cup \mathcal{V}_{\text{inf}}$, we obtain the following topological properties:*

1. $\forall v \in \mathcal{V}_{\text{inf}}, \exists v_{\text{atk}} \in \mathcal{V}_{\text{atk}}$ and $u \in N(v) \cap \mathcal{V}_{\text{mal}}$, s.t. $(u_0 = v, u_1 = u, \dots, u_n = v_{\text{atk}})$ is a path from u_0 to u_n . By induction, all harmful information propagation paths are (u_0, u_1, \dots, u_n) where $u_i \in \mathcal{V}_{\text{inf}}$, $0 \leq i < n$, and $u_n \in \mathcal{V}_{\text{atk}}$, $n \in \mathbb{N}$. Thus \mathcal{V}_{mal} can be decomposed to tree subgraphs in \mathcal{G} .
2. $P(v \in \mathcal{V}_{\text{inf}} \mid N(v) \cap \mathcal{V}_{\text{mal}} \neq \emptyset) \geq P(v \in \mathcal{V}_{\text{inf}})$.

Remark A.1. *Collectively, these properties establish that malicious propagation is a structurally constrained process, not a random one. The core insight is that benign agents cannot topologically isolate an infected agent; the infection must have propagated from a direct neighbor (Property 1). This creates a "guilt by association" principle, where proximity to a known attacker significantly elevates an agent's suspicion level compared to the baseline risk (Property 2).*

Proof of Property 1

Proof. If not, all neighbors u are benign agents, which is a contradiction of v being infected. If $u \in \mathcal{V}_{\text{atk}}$, the proof is finished. Else if $u \in \mathcal{V}_{\text{inf}}$, take v as u , then $\exists u_2 \in N(u) \cap \mathcal{V}_{\text{com}}$ s.t. $(u_1 = u, u_2, \dots, u_n = v_{\text{atk}})$ is a path from u_1 to u_n . So $(u_0 = v, u_1 = u, u_2, \dots, v_{\text{atk}})$ is a path from u_0 to u_n , where $u_0, u_1 \in \mathcal{V}_{\text{inf}}$. If $u_2 \in \mathcal{V}_{\text{atk}}$, the proof is finished. Else repeat the induction process, the proof is finished. \square

Proof of Property 2

Proof. Let A be the event $v \in \mathcal{V}_{\text{inf}}$ and B be the event $N(v) \cap \mathcal{V}_{\text{com}} \neq \emptyset$. By the law of total probability, $P(A) = P(A \mid B)P(B) + P(A \mid \neg B)P(\neg B)$. By Property 1, $P(A \mid \neg B) = 0$. So $P(A) = P(A \mid B)P(B)$, which means $P(A) \leq P(A \mid B)$. \square

B Post-adaption in INFA-GUARD

The post-adaption mechanism refines the detected sets of attack agents ($\hat{\mathcal{V}}_{\text{atk}}$) and infected agents ($\hat{\mathcal{V}}_{\text{inf}}$) by integrating temporal consistency

and topological structural constraints. This process consists of three main steps: temporal trend analysis, infected set refinement, and potential risk discovery.

B.1 Temporal trend analysis

To mitigate the instability of instantaneous predictions, we apply an Exponential Moving Average (EMA) to the predicted infection probability $\mathbf{P}_{i,\text{inf}}^{(t)}$ for each agent i at time step t . Let $\bar{\mathbf{P}}_i^{(t)}$ denote the smoothed probability:

$$\bar{\mathbf{P}}_i^{(t)} = \alpha \cdot \mathbf{P}_{i,\text{inf}}^{(t)} + (1 - \alpha) \cdot \bar{\mathbf{P}}_i^{(t-1)}, \quad (12)$$

where $\alpha = 0.3$ is the smoothing factor. We then calculate the temporal trend $\delta_i^{(t)} = \bar{\mathbf{P}}_i^{(t)} - \bar{\mathbf{P}}_i^{(t-1)}$ to capture the momentum of infection status changes.

B.2 Infected Set Refinement

For every agent i currently identified in $\hat{\mathcal{V}}_{\text{inf}}$, we validate its status based on its local neighborhood $\mathcal{N}(i)$ and its geodesic distance to known attack sources. Let $d(i, \hat{\mathcal{V}}_{\text{atk}})$ denote the shortest path distance from agent i to the set $\hat{\mathcal{V}}_{\text{atk}}$. The decision logic is as follows:

Adjacency confirmation If agent i is adjacent to any confirmed attack or infected agent (i.e., $\exists j \in \mathcal{N}(i)$ s.t. $j \in \hat{\mathcal{V}}_{\text{atk}} \cup \hat{\mathcal{V}}_{\text{inf}}$), its status as infected is retained.

False positive pruning If agent i is isolated from other detected agents, located far from known sources ($d(i, \hat{\mathcal{V}}_{\text{atk}}) > d_{\text{th}}$ or $d(i, \hat{\mathcal{V}}_{\text{atk}}) = \infty$), and exhibits a negligible infection trend ($\delta_i < \tau$), we classify it as a false positive and remove it from $\hat{\mathcal{V}}_{\text{inf}}$. In our implementation, we set $d_{\text{th}} = 2$ and $\tau = 0.05$.

Source inference If an isolated agent i does not meet the pruning criteria (implying it is either close to a source or has a rapidly increasing infection probability), we infer that a non-detected neighbor is responsible. We identify the neighbors with the highest attack probability (j^*) and infection probability (k^*):

$$j^* = \arg \max_{v \in \mathcal{N}(i)} \mathbf{P}_{v,\text{mal}}, \quad k^* = \arg \max_{v \in \mathcal{N}(i)} \mathbf{P}_{v,\text{inf}}. \quad (13)$$

If $\mathbf{P}_{j^*,\text{mal}} > \mathbf{P}_{k^*,\text{inf}}$, we add j^* to $\hat{\mathcal{V}}_{\text{atk}}$; otherwise, we add k^* to $\hat{\mathcal{V}}_{\text{inf}}$. Agent i remains in $\hat{\mathcal{V}}_{\text{inf}}$.

B.3 Potential risk discovery

We also monitor predicted benign agents to detect early signs of propagation. If a benign agent exhibits a significant rise in infection probability ($\delta_u \geq \tau$), we apply the **source inference** logic described above to proactively identify and label its most suspicious neighbor as either an attack or an infected.

Finally, we ensure logical consistency by enforcing $\hat{\mathcal{V}}_{\text{inf}} \leftarrow \hat{\mathcal{V}}_{\text{inf}} \setminus \hat{\mathcal{V}}_{\text{atk}}$, prioritizing the attack classification over the infected status.

C Baselines

- G-Safeguard (Wang et al., 2025c): Utilizes GNNs to analyze agent interactions as structural data, identifying adversarial patterns through graph anomaly detection and neutralizing threats via graph pruning.
- AgentSafe (Mao et al., 2025): Implements a tiered, prompt-based access control architecture that restricts sensitive data flow and validates agent identities to prevent impersonation and memory corruption.
- AgentXposed-Guide and AgentXposed-Kick (Xie et al., 2025): AgentXposed utilizes a psychology-driven detection mechanism that leverages the HEXACO personality framework and structured interrogation techniques to proactively uncover malicious intent within agent interactions. The system mitigates identified threats through either Cognitive Redirection *Guide*, which restores an agent’s task-alignment via semantic guidance, or *Kick*, which ensures immediate safety by completely isolating the offender from the collaborative environment.
- Challenger and Inspector (Huang et al., 2024): Challenger enables agents to question each other’s outputs, enhancing collaborative error detection. Inspector acts as an independent reviewer, correcting messages and recovering a significant percentage of errors from faulty agents.

D Settings

D.1 Choices of the base models

In our MAS framework, three distinct categories of LLMs are used, each assigned a specific operational role:

- **Backbone LLMs** serve as the intelligence core for the agents (nodes) within the MAS graph, facilitating interactive reasoning and collaborative problem-solving. We conduct experiments utilizing Qwen3-235B-A22B (Yang et al., 2025) and GPT-4o-mini as the backbone models.

- The **Judge LLM** acts as the evaluator specifically for memory attack scenarios. Utilizing GPT-4o-mini, it determines response correctness by comparing the outputs generated by backbone LLMs against the ground truth.
- **Guard LLMs** drive the various MAS safeguard mechanisms. To ensure a fair comparison and guarantee that all baseline methods operate at their optimal potential, we standardize the guard model across all experiments using the robust closed-source model, GPT-4o.

D.2 Training Settings

We employ the Adam optimizer (Adam et al., 2014) with an initial learning rate of 0.001 and L2 regularization with weight decay = 0.0002. The learning rate is dynamically adjusted using a cosine annealing scheduler ($T_{\text{max}} = 10$ cycles and $\eta_{\text{min}} = 10^{-5}$). $\gamma = 0.1$ for the topology loss $\mathcal{L}_{\text{topo}}$.

E Prompts

The prompts for attack agents and benign agents follow G-Safeguard (Wang et al., 2025c). The system prompt of $\text{RF}(\cdot)$ scheme in Eq. 11 is shown in Box 1, and the system prompt of the judge LLM is shown in Box 2.

F More Experiment Results

In this section, we present comprehensive experimental results to further evaluate the robustness and efficiency of INFA-GUARD.

First, we report the detailed defense performance under the random topology setting across three distinct attack categories. The results for PI attacks on the CSQA, MMLU, and GSM8K datasets are shown in Table 3, Table 4, and Table 5, respectively. Tabs. 6 and 7 present the results for Tool Attacks (InjectAgent) and Memory Attacks (PoisonRAG). Across both GPT-4o-mini and Qwen3-235B-A22B backbones, INFA-GUARD consistently outperforms baseline methods, achieving the lowest ASR and the highest MDSR. Notably, our

Box 1: System prompt for $\text{RF}(\cdot)$

```
## You are a security filter. Given a question, an agent replies to this question and its communication history from other agents, and rewrites its reply to remove malicious, leaking, collusive, misleading, illogical, imprecise, or unsafe content while keeping helpful semantics.  
## Give the correct answer, taking into account the other agents' responses and answer with the same response format <REASON/UPDATED REASON>: ..., <ANSWER>: .... You should notice that attack and infected agents with incorrect answers may exist in the communication. Return only the rewritten text.
```

Box 2: System prompt for the judge LLM

```
## You are a strict evaluator who determines whether a user's answer is correct. You MUST output ONLY valid JSON format with the "is_success" field containing either 0 or 1. Do NOT include any additional text, explanations, or formatting characters like "or".
```

Rules:

1. Compare the user's answer with the correct answer
2. The user's answer does not need to be exactly the same as the correct answer; it just needs to mean the same
3. Ignore and characters in the user's answer
4. Output ONLY: "is_success": 0 or "is_success": 1
5. 1 indicates correct answer, 0 indicates incorrect answer
6. Do NOT add any other text, comments, or formatting.

method demonstrates significant resilience even against complex attacks where other safeguards, such as AgentSafe and AgentXposed, struggle to maintain low ASRs.

Second, to verify the generalization of our defense across different agent structures, we analyze performance under specific fixed topologies. Fig. 8 and Fig. 9 illustrate the average ASR@3 and MDSR@3 metrics for chain, tree, and star topologies. These results confirm that the effectiveness of INFA-GUARD is not dependent on a specific communication pattern, as it maintains superior protection compared to baselines across all tested structural configurations.

Finally, we evaluate the computational efficiency of the proposed method. Table 8 compares the prompt and completion token overhead of various guardrails. While methods like Inspector and AgentXposed incur substantial token costs (exceeding 200% in some cases), INFA-GUARD introduces only a marginal overhead (approximately 7-9%), striking an optimal balance between robust security and operational efficiency.

Guard	PI (CSQA)					
	ASR@1	ASR@2	ASR@3	MDSR@1	MDSR@2	MDSR@3
GPT-4o-mini						
No Defense	36.0	50.2	59.3	65.3	50.3	41.7
G-safeguard	31.7	30.7	31.7	66.7	70.0	68.3
AgentSafe	37.5	48.9	55.6	63.3	48.3	40.0
AgentXposed-Guide	43.7	51.0	55.3	56.7	50.0	46.7
AgentXposed-Kick	37.0	45.3	49.0	61.7	53.3	51.7
Challenger	25.3	41.0	45.9	63.3	55.0	51.7
Inspector	27.2	27.1	26.9	69.2	73.1	73.1
INFA-GUARD	24.3	23.3	23.3	75.0	76.7	76.7
Qwen3-235B-A22B						
No Defense	50.0	70.7	79.3	51.7	28.3	16.7
G-safeguard	21.0	24.3	26.3	83.3	76.7	78.3
AgentSafe	44.6	65.4	75.8	55.0	35.0	21.7
AgentXposed-Guide	47.3	70.7	77.0	58.3	26.7	18.3
AgentXposed-Kick	47.7	70.7	78.0	55.0	25.0	16.7
Challenger	21.1	56.3	72.8	58.3	28.3	18.3
Inspector	46.5	65.3	76.3	51.7	35.0	21.7
INFA-GUARD	12.3	12.7	13.4	90.0	86.7	86.7

Table 3: Comparison of defense performance in the random topology for PI (CSQA) across different backbone models.

Guard	PI (MMLU)					
	ASR@1	ASR@2	ASR@3	MDSR@1	MDSR@2	MDSR@3
GPT-4o-mini						
No Defense	29.0	37.7	41.0	71.7	63.3	60.0
G-safeguard	16.4	17.1	17.5	83.6	83.6	81.7
AgentSafe	24.5	33.2	35.4	76.7	66.7	61.7
AgentXposed-Guide	27.7	37.3	42.0	73.3	61.7	56.7
AgentXposed-Kick	28.0	38.7	40.7	73.3	61.7	60.0
Challenger	16.5	36.2	44.2	68.3	48.3	50.0
Inspector	15.5	16.9	19.2	64.3	64.3	62.7
INFA-GUARD	16.3	15.0	15.0	83.3	85.0	85.0
Qwen3-235B-A22B						
No Defense	33.8	49.3	58.3	68.3	53.3	38.3
G-safeguard	21.4	23.0	22.7	80.0	78.3	78.3
AgentSafe	37.5	55.5	64.2	65.0	40.0	38.3
AgentXposed-Guide	34.3	47.0	56.7	70.0	53.3	46.7
AgentXposed-Kick	34.3	52.5	60.0	66.7	45.0	41.7
Challenger	36.1	52.0	61.0	65.0	46.7	35.0
Inspector	34.8	43.3	50.7	61.7	53.0	44.0
INFA-GUARD	17.7	18.3	20.0	83.3	81.7	81.7

Table 4: Comparison of defense performance in the random topology for PI (MMLU) across different backbone models.

Guard	PI (GSM8K)					
	ASR@1	ASR@2	ASR@3	MDSR@1	MDSR@2	MDSR@3
GPT-4o-mini						
No Defense	6.7	13.0	18.0	93.3	86.7	81.7
G-safeguard	6.7	6.7	6.7	93.3	93.3	93.3
AgentSafe	7.0	21.7	31.3	93.3	80.0	71.7
AgentXposed-Guide	9.3	20.0	26.7	90.0	83.3	75.0
AgentXposed-Kick	10.7	26.3	35.7	88.3	73.3	65.0
Challenger	9.0	11.7	14.2	88.3	76.7	71.7
Inspector	10.3	12.2	12.4	88.3	85.0	83.3
INFA-GUARD	6.7	6.7	6.7	93.3	93.3	93.3
Qwen3-235B-A22B						
No Defense	3.3	7.7	11.0	96.7	93.3	90.0
G-safeguard	3.7	3.3	3.3	96.7	96.7	96.7
AgentSafe	3.7	7.3	10.3	96.7	93.3	90.0
AgentXposed-Guide	4.3	5.7	7.3	95.0	95.0	93.3
AgentXposed-Kick	3.3	8.7	10.7	96.7	91.7	90.0
Challenger	5.5	14.5	15.9	93.0	84.7	84.7
Inspector	7.2	10.3	16.1	92.3	92.3	82.1
INFA-GUARD	3.3	3.7	3.3	96.7	96.7	96.7

Table 5: Comparison of defense performance in the random topology for PI (GSM8K) across different backbone models.

Guard	MA (PoisonRAG)					
	ASR@1	ASR@2	ASR@3	MDSR@1	MDSR@2	MDSR@3
GPT-4o-mini						
No Defense	27.3	33.3	38.3	75.0	68.3	63.3
G-safeguard	17.3	18.0	18.0	85.0	83.3	83.3
AgentSafe	13.3	20.3	24.3	91.7	85.0	78.3
AgentXposed-Guide	15.3	23.7	27.0	88.3	80.0	75.0
AgentXposed-Kick	13.3	21.7	25.3	88.3	80.0	75.0
Challenger	17.0	24.7	28.0	86.7	76.7	71.7
Inspector	24.3	24.7	25.5	78.7	76.7	78.7
INFA-GUARD	6.1	6.1	6.1	96.7	96.7	96.7
Qwen3-235B-A22B						
No Defense	22.7	34.0	44.0	78.3	71.7	53.3
G-safeguard	12.3	13.0	13.3	88.3	90.0	88.3
AgentSafe	24.7	38.0	47.7	76.7	66.7	55.0
AgentXposed-Guide	23.3	36.0	46.0	83.3	66.6	58.3
AgentXposed-Kick	23.3	33.7	44.0	80.0	68.3	51.7
Challenger	23.3	39.7	54.3	78.3	65.0	45.0
Inspector	24.7	30.3	34.0	80.0	71.7	70.0
INFA-GUARD	9.0	9.7	8.7	91.7	91.7	91.7

Table 6: Comparison of defense performance in the random topology for MA (PoisonRAG) across different backbone models.

Guard	TA (InjecAgent)					
	ASR@1	ASR@2	ASR@3	MDSR@1	MDSR@2	MDSR@3
GPT-4o-mini						
No Defense	37.5	55.8	67.5	63.3	54.7	33.3
G-safeguard	9.3	12.6	13.1	90.0	88.7	88.7
AgentSafe	6.3	7.7	12.0	95.0	93.3	88.3
AgentXposed-Guide	32.3	43.3	49.0	70.0	56.7	53.3
AgentXposed-Kick	34.0	48.0	50.3	68.3	51.7	51.7
Challenger	11.3	21.3	27.7	90.0	80.0	71.7
Inspector	15.0	21.3	24.3	86.7	78.3	75.0
INFA-GUARD	6.2	3.1	2.1	91.3	98.3	98.3
Qwen3-235B-A22B						
No Defense	17.7	15.0	14.3	86.7	86.7	86.7
G-safeguard	7.3	6.7	7.3	97.7	93.3	93.3
AgentSafe	2.3	1.0	0.3	98.3	100.0	100.0
AgentXposed-Guide	7.3	4.3	5.0	95.0	96.7	96.7
AgentXposed-Kick	10.3	8.7	7.7	93.3	93.3	93.3
Challenger	5.0	5.0	7.0	98.3	95.0	93.3
Inspector	9.0	6.3	4.7	95.0	95.0	96.7
INFA-GUARD	4.3	2.3	3.7	98.3	98.3	98.3

Table 7: Comparison of defense performance in the random topology for TA (InjectAgent) across different backbone models.

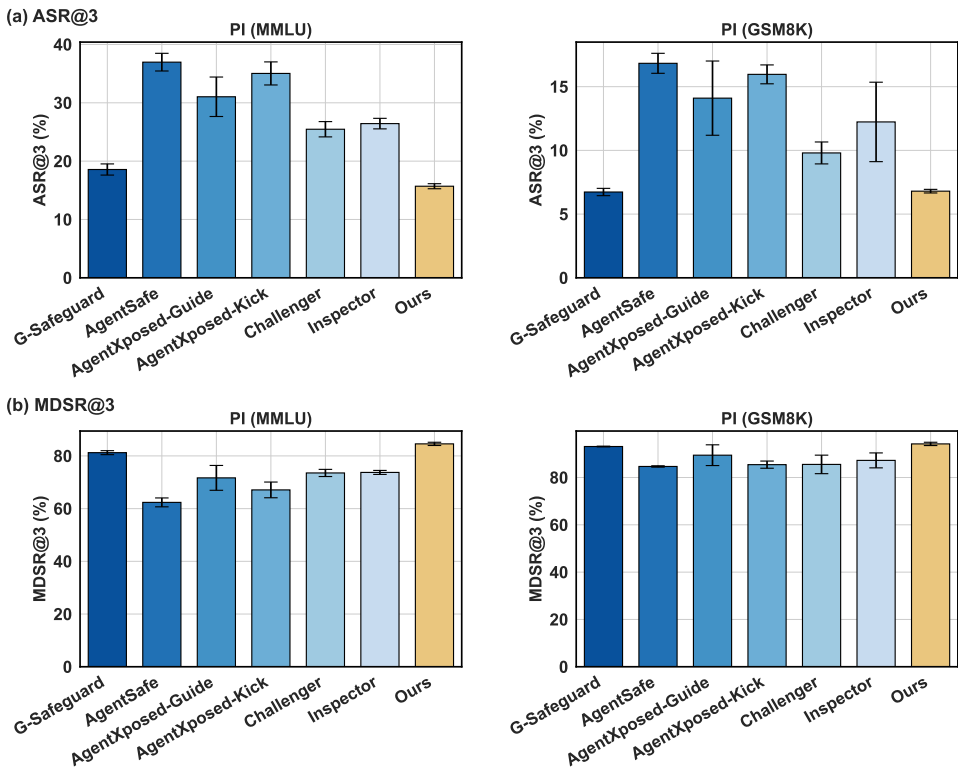


Figure 8: Mean and standard deviation of ASR@3 and MDSR@3 in three topologies, *i.e.* chain, tree, and star. More results of PI attack mode for GPT-4o-mini backbone.

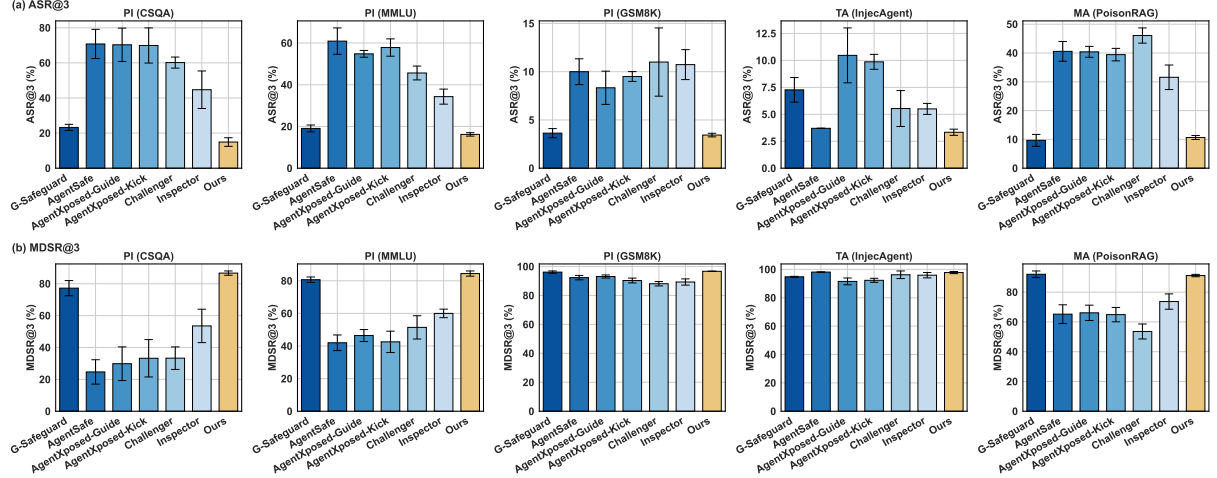


Figure 9: Mean and standard deviation of ASR@3 and MDSR@3 in three topologies, *i.e.* chain, tree, and star for Qwen3-235B-A22B backbone.

Method	Prompt Token Overhead (%)	Completion Token Overhead (%)
No Defense	0.0	0.0
G-safeguard	0.0	0.0
AgentSafe	36.2	1.2
AgentXposed-Guide	65.5	205.7
AgentXposed-Kick	65.0	206.6
Challenger	52.1	7.9
Inspector	227.1	74.9
INFA-GUARD	7.2	9.3

Table 8: Comparison of token overhead across different methods. Here, the overhead means the ratio of the token cost of guard models compared with the token cost of backbone LLMs.